

## Simultaneous propagation of short different-wavelength optical pulses

M. J. Konopnicki\* and J. H. Eberly

*Department of Physics and Astronomy, The University of Rochester,  
Rochester, New York 14627*

(Received 20 October 1980; revised manuscript received 6 April 1981)

The propagation of two short different-wavelength optical pulses in three-level absorbers is studied. Combined numerical and analytic techniques are used to solve the three-level Maxwell-Bloch equations that provide the semiclassical description of the problem. The electric field in the model studied consists of two copropagating plane waves, each of which is in near resonance with a transition in the absorber. A new conservation law, holding in the absence of relaxation mechanisms, and independent of particular values of fields and detunings, is given. It is an analog of the law expressing conservation of the Bloch vector length known for two-level atoms. The possibility of simultaneous lossless propagation of the two optical pulses is established. New analytic solutions having the form of simultaneous different-wavelength optical solitons have been found. These pairs of solitons are called simultons. In order for simulton propagation to occur, both the pulses and the medium have to be prepared in a manner determined by the medium's physical parameters. The conditions for such preparation are given. Simultons are predicted to be distinct from the single-wavelength multiple-pulse solutions resulting from large-area-pulse breakup known in two-level absorbers, as well as from two-photon self-induced transparency. Results of numerical experiments on different-wavelength simultaneous propagation are also presented and indicate that simultaneous propagation may also be obtained under less stringent conditions than those predicted by the analytic solutions. Evidence of pulse evolution and breakup is seen.

### I. INTRODUCTION

In this work we describe results of theoretical studies of the propagation of short optical pulses through material media. We concentrate on the situation in which the light-matter interaction is near resonant. We extend previous work by treating a system consisting of a three-level atom interacting with two different-wavelength optical pulses, each of which is on or near resonance with one of the dipole-allowed transitions in the medium.

When the radiation is in the form of nearly resonant pulses whose duration is shorter than all of the relevant atomic relaxation times, the polarization induced in the medium will show a definite phase relationship with the applied radiation. Such an interaction will be described as being coherent. Coherent resonant interactions may be

divided into two groups, those dealing with atomic excitation at a single space point, and those dealing with propagation effects (in which the extent of the atomic absorber makes it necessary to consider spatial changes in the radiation field). We are concerned with the latter in this paper.

The principal resonant atomic model studied to date is the two-level atom. Within the semiclassical approach<sup>1</sup> the propagation problem in a two-level atomic medium has self-consistent solutions<sup>2</sup> to both the coupled Maxwell and Schrödinger or Heisenberg equations. Under the usual slowly varying envelope approximation (SVEA) and rotating-wave approximation (RWA) a simplified set of equations is obtained, usually referred to as the Maxwell-Bloch equations<sup>1</sup> (for a two-level atom). Such a description has been adequate in propagation studies in absorbing<sup>2-4</sup> and amplifying<sup>3-6</sup> media. In particular, it has predicted the

existence of lossless and shape-preserving solutions for both absorbing and amplifying media,<sup>2-5</sup> and has allowed one to predict trends in pulse evolution by using the so-called area theorem<sup>1,2</sup> or the area-energy formulation of the propagation problem.<sup>6</sup> For an absorber, the single pulse asymptotic solutions are given by the celebrated sech  $2\pi$  pulse of self-induced transparency.<sup>2</sup> Evolution (with propagation) of nonsech pulses toward the asymptotic sech form can involve considerable pulse reshaping and breakup.<sup>1-4</sup> Although many analytic solutions of the Maxwell-Bloch equations are known, numerical solutions, even for the simplified two-level case, are the rule rather than the exception.

The situation becomes more involved if one wants to consider atom-radiation interactions for cases involving a larger number of atomic energy levels, different-wavelength fields, or both. In the spirit of the simplest two-level propagation formulation, in Sec. II we describe the equations capable of handling the resonant different-wavelength propagation problem in a three-level absorber. We will refer to these as the three-level Maxwell-Bloch equations. In order to make the formulation more suitable for numerical work, we have elected to work with real and imaginary parts of Rabi frequencies, rather than with the usual envelope-phase representation.<sup>5</sup> Although the concepts involved are quite clear, the formalism has never been both stated and solved for the three-level propagation problem without further simplifications.

Many papers<sup>7,8</sup> have been devoted to studies of the dynamics alone of more complicated  $N$ -level systems ( $N \geq 3$ ) interacting with the fields of  $(N - 1)$  lasers, where each field was characterized by a constant envelope function. Work by Cook and Shore<sup>8</sup> deserves special attention, being the first attempt to find exact RWA solutions for the  $N$ -level atom's evolution under the influence of several fields with time-dependent envelopes. That work was further generalized by Konopnicki.<sup>9</sup>

The two-photon (different-wavelengths) self-induced-transparency work of Tan-no *et al.*<sup>10,11</sup> (and their work on the coherent Raman problem) starts with a full description of the three-level different-wavelength propagation problem, only to simplify it immediately by the technique of adiabatic elimination,<sup>1</sup> obtaining at the end an effective two-level-atom description, with a bilinear two-photon Rabi frequency. For a three-level system simplified in this way, asymptotic Lorentzian solutions capable of steady-state propagation are found.<sup>10</sup> Regarding the full different-wavelength

resonant propagation problem, with the exception of preliminary work of Cardimona and Stroud,<sup>12</sup> the present paper seems to be the first attempt.<sup>9,13</sup>

In spite of the relative complexity of the mathematical description we are dealing with, it is possible to make some analytic progress. In Sec. II we will give a new conservation law, an analog of the Bloch vector length conservation known for two-level atoms, but in the present case unrelated to probability conservation. We will also obtain solutions to the full set of on-resonance three-level Maxwell-Bloch equations. These have the character of simultaneous different-wavelength optical solitons. We will call them simultons for the sake of brevity. For simulton propagation to occur, it is necessary that certain conditions, imposed on the initial preparation of both the pulses and the medium, and determined by the medium's physical parameters, are satisfied. The conditions are listed and their implications discussed in the same section. As a rule, the individual areas of the soliton members of a simulton will be different from  $2\pi$ . Simultons are quite distinct from the soliton solutions of both the usual<sup>1-3</sup> and the two-photon self-induced-transparency problems.<sup>10,11</sup> These points are raised in Sec. III.

In Sec. IV we report numerical results dealing with simultaneous different-wavelength propagation. These results will show that, although the analytic results of Sec. III have limitations to their strict validity, there are some indications that simultaneous propagation can be obtained under more general and less stringent conditions. The numerical solutions show evidence of pulse evolution and/or breakups, possibly indicative of some global relationships governing the propagation problem at hand. In the Appendix we will give, for the sake of completeness, details of obtaining the full set of three-level Maxwell-Bloch equations used in this paper.

## II. SEMICLASSICAL DESCRIPTION OF DIFFERENT-WAVELENGTH COHERENT PROPAGATION OF SHORT OPTICAL PULSES IN A THREE-LEVEL ATOMIC MEDIUM

Within this work we will deal with atoms that consist of three discrete energy levels only, numbered 1, 2, and 3, with their respective energies  $E_1$ ,  $E_2$ , and  $E_3$ . Depending on the energy eigenvalues  $\{E_j\}$  associated with given levels  $\{j\}$ , and on the

allowed dipole transitions, we will deal with three distinct configurations of levels, namely, "cascade", "Λ", and "V". These configurations are shown in Fig. 1, where arrows connecting any two levels represent allowed dipole transitions. We choose to label the levels in such a way that the level that is dipole connected to both of the remaining levels is always denoted as level 2, and the lower of the other two is denoted level 1. The electric-field vector  $\vec{E}$  is treated as a purely classical object. We assume that it is the sum of two quasimonochromatic plane waves copropagating along the  $z$  axis with possibly different velocities:

$$\vec{E}(z,t) = \vec{E}_a(z,t) + \vec{E}_b(z,t), \quad (1a)$$

$$\vec{E}_a(z,t) = \vec{e}_a \mathcal{E}_a(z,t) e^{-i(\omega_a t - k_a z)} + \text{c.c.}, \quad (1b)$$

and a corresponding expression for  $\vec{E}_b(z,t)$ .

Here  $\vec{e}_a$  and  $\vec{e}_b$  denote possibly complex unit polarization vectors,  $\omega_a$  and  $\omega_b$  are their respective carrier frequencies, and  $k_a$  and  $k_b$  denote their wave vectors in the vacuum, i.e.,  $\omega_a/c$  and  $\omega_b/c$ , respectively.  $\mathcal{E}_a(z,t)$  and  $\mathcal{E}_b(z,t)$  are the generally complex amplitudes of the two waves, and are assumed to be slowly varying functions of  $z$  and  $t$  in the following sense:

$$\frac{1}{\omega_a} \left| \frac{\partial \mathcal{E}_a(z,t)}{\partial t} \right| \ll \left| \mathcal{E}_a(z,t) \right|, \quad (2)$$

$$\frac{1}{k_a} \left| \frac{\partial \mathcal{E}_a(z,t)}{\partial z} \right| \ll \left| \mathcal{E}_a(z,t) \right|.$$

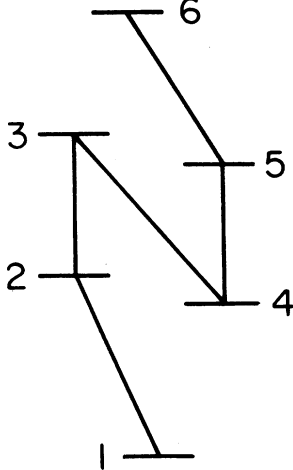


FIG. 1. Possible configurations of energy levels in an atom. Arrows indicate the allowed dipole transitions ( $1 \leftrightarrow 2$ ) and ( $2 \leftrightarrow 3$ ), etc.

The electric-field vector  $\vec{E}$ , given by (1), obeys the following Maxwell equation:

$$\left[ \frac{\partial^2}{\partial z^2} - \frac{1}{c^2} \frac{\partial^2}{\partial t^2} \right] \vec{E}(z,t) = \frac{4\pi}{c^2} \frac{\partial^2 \vec{P}(z,t)}{\partial t^2}, \quad (3)$$

where  $\vec{P}(z,t)$  is the induced macroscopic polarization vector, and  $c$  is the velocity of light in vacuum.

The three-level atom is treated as a quantum object. The Hamiltonian operator  $\hat{H}$  of the three-level atomic system in the Schrödinger picture is

$$\hat{H} = \hat{H}_A - \vec{d} \cdot \vec{E}(z,t), \quad (4)$$

where  $\hat{H}_A$  denotes the Hamiltonian operator of the atom in the absence of the applied field,  $\vec{d}$  is the electric-dipole-moment operator, and  $\vec{E}(z,t)$  is to be evaluated at the position of the dipole. A detailed knowledge of the free Hamiltonian is not necessary. Its eigenvalues are defined as

$$\hat{H}_A |j\rangle = E_j |j\rangle, \quad j=1,2,3 \quad (5)$$

where  $\{E_j\}$  denotes the energy spectrum of the free atom.

Introducing the usual transition-projection operators  $\hat{\sigma}_{ij}$  as follows:

$$\hat{\sigma}_{ij} = |i\rangle \langle j|, \quad i,j=1,2,3 \quad (6)$$

we can describe the behavior of the atom under the influence of the applied fields by giving the Heisenberg picture equations of motion for the  $\hat{\sigma}_{ij}$ 's

$$\frac{\partial}{\partial t} [\hat{\sigma}_{ij}(t)] = i\omega_{ij} \hat{\sigma}_{ij}(t) + \frac{i}{\hbar} \sum_k [\vec{d}_{jk} \hat{\sigma}_{ik}(t) - \vec{d}_{ki} \hat{\sigma}_{kj}(t)] \cdot \vec{E}(z,t), \quad (7)$$

where  $\omega_{ij}$  is the circular frequency associated with transition ( $i \leftrightarrow j$ ):

$$\omega_{ij} = \frac{1}{\hbar} (E_i - E_j), \quad (8)$$

and  $\vec{d}_{ij}$  is given by

$$\vec{d}_{ij} = \langle i | \vec{d} | j \rangle. \quad (9)$$

As it is outlined in the Appendix, Eqs. (7) can be simplified leading to the following equations of motion involving slowly varying real quantities only:

$$\dot{v}_{12} = \Delta_a u_{12} + R_{12} w_{21} - \frac{1}{2} R_{23} u_{13} - \frac{1}{2} U_{23} v_{13}, \quad (10a)$$

$$\dot{u}_{12} = -\Delta_a v_{12} - U_{12} w_{21} + \frac{1}{2} R_{23} v_{13} - \frac{1}{2} U_{23} u_{13}, \quad (10b)$$

$$\dot{v}_{23} = \Delta_b u_{23} + R_{23} w_{32} + \frac{1}{2} R_{12} u_{13} + \frac{1}{2} U_{12} v_{13}, \quad (10c)$$

$$\dot{u}_{23} = -\Delta_b v_{23} - U_{23} w_{32} - \frac{1}{2} R_{12} v_{13} + \frac{1}{2} U_{12} u_{13}, \quad (10d)$$

$$\begin{aligned} \dot{v}_{13} = & (\Delta_a + \Delta_b) u_{13} + \frac{1}{2} R_{12} u_{23} - \frac{1}{2} R_{23} u_{12} \\ & - \frac{1}{2} U_{12} v_{23} + \frac{1}{2} U_{23} v_{12}, \end{aligned} \quad (10e)$$

$$\begin{aligned} \dot{u}_{13} = & -(\Delta_a + \Delta_b) v_{13} - \frac{1}{2} R_{12} v_{23} + \frac{1}{2} R_{23} v_{12} \\ & - \frac{1}{2} U_{12} u_{23} + \frac{1}{2} U_{23} u_{12}, \end{aligned} \quad (10f)$$

$$\dot{r}_{11} = \frac{1}{2} R_{12} v_{12} - \frac{1}{2} U_{12} u_{12}, \quad (10g)$$

$$\begin{aligned} \dot{r}_{22} = & -\frac{1}{2} R_{12} v_{12} + \frac{1}{2} U_{12} u_{12} + \frac{1}{2} R_{23} v_{23} \\ & - \frac{1}{2} U_{23} u_{23}, \end{aligned} \quad (10h)$$

$$\dot{r}_{33} = -\frac{1}{2} R_{23} v_{23} + \frac{1}{2} U_{23} u_{23}, \quad (10i)$$

where  $w_{21}$  and  $w_{32}$  are atomic inversions defined by

$$w_{21} = r_{22} - r_{11}, \quad (11a)$$

$$w_{32} = r_{33} - r_{22}. \quad (11b)$$

It should be pointed out that Eqs. (10) have been written for the cascade configuration of atomic energy levels. In particular, we have assumed that the applied field of the carrier frequency  $\omega_a$  is on or near resonance with the allowed dipole transition  $1 \leftrightarrow 2$ , i.e.,  $\omega_a \approx \omega_{21}$ . Similarly, the field of the carrier frequency  $\omega_b$  is on or near resonance with the transition  $2 \leftrightarrow 3$ . In a separate paper<sup>14</sup> we have provided simple rules that allow one to obtain the equations appropriate for other configurations of energy levels directly from the equations used here.

Under the assumptions introduced so far, Eqs. (10) constitute a full description of the interaction between a three-level atom and two optical pulses if all incoherent relaxation mechanisms are ignored. We will refer to Eqs. (10) as the three-level Bloch equations. In Eqs. (10) one can readily identify the terms that would describe just a two-level atom interacting with a single pulse. The two-level (nearly) resonant parts of our three-level atom (transitions 1-2 and 2-3) are not independent. This is first of all due to the obvious fact that each of the "two-level atoms" shares level 2 with the other one. Both transitions compete for the population of level 2, even though they operate at different frequencies. Moreover, the two-level atoms will be additionally coupled through terms involving  $u_{13}$

and  $v_{13}$ , the real and imaginary (slowly varying) parts of the two-photon density-matrix element induced together by both (nearly) resonant fields of carrier frequencies  $\omega_a$  and  $\omega_b$ .

Despite the intercouplings of the two two-level atoms, it is possible to obtain from equations of motion (10) the following conservation law<sup>9</sup>:

$$\begin{aligned} v_{12}^2 + u_{12}^2 + v_{23}^2 + u_{23}^2 + v_{13}^2 + u_{23}^2 \\ + 2(r_{11}^2 + r_{12}^2 + r_{33}^2) = C, \end{aligned} \quad (12)$$

reminiscent of Bloch: vector conservation<sup>1</sup> in a single two-level atom. Here  $C$  is a constant whose value is determined by the initial conditions of the problem. Related expressions involving only  $r_{ij}$ 's or  $\sigma_{ij}$ 's can also be derived.<sup>9</sup> It should also be noted that similar relations dealing with two-photon processes<sup>10,11</sup> are subsets of the conservation law (12). The conservation law (12) holds for all times, and is independent of the instantaneous Rabi frequencies and detunings of the problem. The conservation law (12), together with the familiar law of probability conservation  $\sum_i r_{ii} = 1$ , impose considerable constraints on the possible values of the three-level Bloch variables.<sup>15</sup>

The induced macroscopic polarization vector  $\vec{P}(z, t)$  can be written as

$$\vec{P}(z, t) = N \langle \vec{d}_{12} \sigma_{12} + \vec{d}_{21} \sigma_{21} + \vec{d}_{23} \sigma_{23} + \vec{d}_{32} \sigma_{32} \rangle, \quad (13)$$

where  $N$  denotes the density of atoms, and  $\langle \dots \rangle$  denotes averaging over the Maxwellian velocity distribution of the atoms.

Once again, invoking the assumptions of the Appendix, we can obtain the reduced Maxwell equations for the problem,

$$\left[ \frac{\partial}{\partial z} + \frac{\partial}{\partial(ct)} \right] R_{12}(z, t) = \frac{1}{2} G_a \langle v_{12} \rangle, \quad (14a)$$

$$\left[ \frac{\partial}{\partial z} + \frac{\partial}{\partial(ct)} \right] U_{12}(z, t) = -\frac{1}{2} G_a \langle u_{12} \rangle, \quad (14b)$$

$$\left[ \frac{\partial}{\partial z} + \frac{\partial}{\partial(ct)} \right] R_{23}(z, t) = \frac{1}{2} \beta G_a \langle v_{23} \rangle, \quad (14c)$$

$$\left[ \frac{\partial}{\partial z} + \frac{\partial}{\partial(ct)} \right] U_{23}(z, t) = -\frac{1}{2} \beta G_a \langle u_{23} \rangle, \quad (14d)$$

where the following definitions have been used:

$$G_a = \frac{4\pi N d_a^2 \omega_a}{\hbar c}, \quad (15a)$$

$$\beta = \frac{d_b^2 \omega_b}{d_a^2 \omega_a}, \quad (15b)$$

$$d_{a,b} = |\vec{\epsilon}_{a,b} \cdot \vec{d}_{12,23}|. \quad (16)$$

Note that  $G$  is the primitive "gain" coefficient (gain times linewidth per unit length) of Icevigi and Lamb<sup>5</sup> and  $\beta$  is the ratio of the oscillator strengths of the two transitions.

The coupled three-level Maxwell-Bloch equations (10) and (14) form a complete semiclassical description of the resonant different-wavelength propagation problem we are dealing with. Except for Refs. 9 and 13, to the best of our knowledge, the full set of resonant Maxwell-Bloch equations have never been treated before either analytically or numerically without major simplifications, such as the adiabatic elimination of the off-diagonal terms involving level 2.

### III. SIMULTONS: DEFINITION AND ANALYTIC RESULTS

In this section we will explore the possibility of the existence of solutions to the coupled Maxwell-Bloch equations (10) and (14) that would depend on both  $t$  and  $z$  variables through the argument  $\zeta = t - z/V$  only. Such solutions would represent two different-wavelength pulses traveling together (with the same velocity  $V$ ) through a three-level absorber. We could describe such solutions as "simultaneous different-wavelength solitons," or "simultons" for the sake of brevity. This new name allows us to differentiate this case from the situations when one deals with two-level pulse train solutions or several optical solitons of the same wavelength (such as exist from the breakup of a large area single pulse), known in studies of self-induced transparency. The latter we may describe as multiple (*not* simultaneous) single-wavelength solitons.

Although this is not required by the general definition of a three-level simulton solution, within this section we will restrict ourselves to Rabi frequencies that are real and given by the shape-preserving expressions

$$R_{12}(\zeta) = \alpha_1 \Omega(\zeta), \quad (17a)$$

$$R_{23}(\zeta) = \alpha_2 \Omega(\zeta). \quad (17b)$$

We will occasionally refer to pulses (17) as generalized Cook-Shore pulses.<sup>8,9</sup> We will further assume that Doppler-broadening and laser line center-

atomic line center detunings can be ignored. The Maxwell equations for this case will simply become

$$\alpha_1 \left[ \frac{1}{V} - \frac{1}{c} \right] \dot{\Omega} = -\frac{1}{2} G_a v_{12}, \quad (18a)$$

$$\alpha_2 \left[ \frac{1}{V} - \frac{1}{c} \right] \dot{\Omega} = -\frac{1}{2} \beta G_a v_{23}, \quad (18b)$$

where the dot ( $\dot{\cdot}$ ) denotes a derivative with respect to the local pulse-time variable  $\zeta$ . The time derivatives in the three-level Bloch equations (10) can also be trivially changed to derivatives with respect to  $\zeta$ .  $\alpha_1$  and  $\alpha_2$  are the relative amplitudes of the pulses.

Comparing the two Maxwell equations (18), we see that restricting our attention to generalized Cook-Shore pulses only imposes a condition on the atomic variables and relative pulse amplitudes, namely,

$$\frac{v_{12}}{\alpha_1} = \frac{v_{23}}{\beta \alpha_2}. \quad (19)$$

We should also note that, in fact, we are dealing with a single differential equation for the variable  $\Omega(\zeta)$ , while the other Maxwell equation is replaced by the condition (19).

We will postulate now the following simulton solution of the Maxwell-Bloch equations (10) and (18) for generalized Cook-Shore pulses (17):

$$\Omega(\zeta) = \frac{2}{\tau} \operatorname{sech} \left[ \frac{\zeta}{\tau} \right], \quad (20a)$$

$$v_{12}(\zeta) = a_1 \operatorname{sech} \left[ \frac{\zeta}{\tau} \right] \tanh \left[ \frac{\zeta}{\tau} \right], \quad (20b)$$

$$v_{23}(\zeta) = a_2 \operatorname{sech} \left[ \frac{\zeta}{\tau} \right] \tanh \left[ \frac{\zeta}{\tau} \right], \quad (20c)$$

$$w_{21}(\zeta) = a_3 + a_4 \operatorname{sech}^2 \left[ \frac{\zeta}{\tau} \right], \quad (20d)$$

$$w_{32}(\zeta) = a_5 + a_6 \operatorname{sech}^2 \left[ \frac{\zeta}{\tau} \right], \quad (20e)$$

$$u_{13}(\zeta) = a_7 \operatorname{sech}^2 \left[ \frac{\zeta}{\tau} \right], \quad (20f)$$

where  $\tau$  denotes the pulse length and  $a_3$  and  $a_5$  are the initial inversions  $w_{21}(\zeta = -\infty)$  and  $w_{32}(\zeta = -\infty)$ , respectively. Substituting relations (20) into (10), and assuming that  $\alpha_1$  and  $\alpha_2$  are known, we solve the resulting system of linear

homogeneous algebraic equations<sup>16</sup> in terms of  $a_3$  obtaining

$$a_1 = -2\alpha_1 a_3, \quad (21a)$$

$$a_2 = -2 \frac{\alpha_1^2}{\alpha_2} a_3, \quad (21b)$$

$$a_4 = -\alpha_1^2 a_3, \quad (21c)$$

$$a_5 = \frac{\alpha_1^2}{\alpha_2^2} a_3, \quad (21d)$$

$$a_6 = -\alpha_1^2 a_3, \quad (21e)$$

$$a_7 = \alpha_1 \alpha_2 \left[ 1 - \frac{\alpha_1^2}{\alpha_2^2} \right] a_3, \quad (21f)$$

with the condition

$$a_1^2 + a_2^2 = 4. \quad (22)$$

Alternatively, we can find the solutions

$$a_1 = -2\alpha_1 a_3, \quad (23a)$$

$$a_2 = 2\alpha_2 a_3, \quad (23b)$$

$$a_4 = -(1 + \alpha_1^2) a_3, \quad (23c)$$

$$a_5 = -a_3, \quad (23d)$$

$$a_6 = (1 + \alpha_2^2) a_3, \quad (23e)$$

$$a_7 = 2\alpha_1 \alpha_2 a_3, \quad (23f)$$

under the condition

$$\alpha_1^2 + \alpha_2^2 = 1. \quad (24)$$

At this point, we are dealing with two classes of equally possible solutions of the Bloch equations (10) when the applied pulses are given by (17) and  $\Omega(\xi)$  by (20a). The Bloch equations (10) by themselves will not provide us with any indication that one of the solutions may be preferable over another. This situation changes when we try to establish the compatibility of solutions (21) and (23) with the Maxwell equations.

We consider first the case  $\alpha_1^2 + \alpha_2^2 = 4$  and the cascade-configuration Maxwell equations (18). Using (20) and (21), and substituting into (18) we obtain

$$\begin{aligned} \alpha_1 \left[ \frac{1}{V} - \frac{1}{c} \right] \left[ -\frac{2}{\tau^2} \operatorname{sech} \left[ \frac{\xi}{\tau} \right] \tanh \left[ \frac{\xi}{\tau} \right] \right] \\ = \alpha_1 G_a a_3 \operatorname{sech} \left[ \frac{\xi}{\tau} \right] \tanh \left[ \frac{\xi}{\tau} \right], \end{aligned} \quad (25a)$$

$$\begin{aligned} \alpha_2 \left[ \frac{1}{V} - \frac{1}{c} \right] \left[ -\frac{2}{\tau^2} \operatorname{sech} \left[ \frac{\xi}{\tau} \right] \tanh \left[ \frac{\xi}{\tau} \right] \right] \\ = \frac{\alpha_1}{\alpha_2^2} G_a \beta a_3 \operatorname{sech} \left[ \frac{\xi}{\tau} \right] \tanh \left[ \frac{\xi}{\tau} \right]. \end{aligned} \quad (25b)$$

Comparing coefficients of both sides of (25a) we get

$$\frac{1}{\tau^2} = -\frac{1}{2} \frac{G_a a_3}{1/V - 1/c}. \quad (26)$$

We should note that in order to have  $\tau^2 > 0$  and  $V < c$ , we have to require that  $a_3 < 0$ . Since  $a_3$  is the initial inversion for levels 1 and 2, and we are interested in absorbers,  $a_3$  is clearly negative in all cases considered here.

In common with two-level self-induced transparency,<sup>1-3</sup> the problem at hand has one free parameter. Thus we can treat (26) as a definition of  $\tau$  with given velocity  $V$ , or conversely, as a definition of  $V$  when the pulse width is given.

We obtain another relation among the parameters,

$$\frac{\alpha_2^2}{\beta \alpha_1^2} = 1, \quad (27)$$

by dividing (25a) by (25b). Relation (27) represents another restriction on the possible relative amplitudes of the pulses, expressed in terms of the physical parameters of the problem (dipole moments, carrier frequencies). We can obtain from (22) and (27) the following expressions for amplitudes  $\alpha_1$  and  $\alpha_2$ :

$$\alpha_1^2 = \frac{4}{1 + \beta}, \quad (28a)$$

$$\alpha_2^2 = \frac{4\beta}{1 + \beta}. \quad (28b)$$

Relations (28) express the fact that, in a cascade medium characterized by parameter  $\beta$ , only such generalized Cook-Shore pulses whose amplitudes are given by (28) and profiles by (17) and (20), will be potentially able to propagate as a three-level simulton. Conditions (28) will not, however, be sufficient to secure such propagation.

Another factor that still has to be considered is the proper initial preparation of the medium, implied by the explicit connection (21d) between the initial inversions  $a_3$  and  $a_5$ . One of the consequences of the relation (21d) is the fact that for  $a_3$ ,  $\alpha_1$  and  $\alpha_2$  all nonvanishing, simulton propagation is not possible in a cascade medium that was ini-

tially in the ground state ( $a_3 = -1$ ), as that would imply that the inversion between levels 3 and 1,

$$w_{31} = w_{21} + w_{32} ,$$

is initially less than  $-1$ , resulting in a contradiction. Thus simulton propagation is, in a cascade atom, possible only for an appropriate initial mixed state, in which the initial inversions are connected by relation (21d).

One should also note that changes in both inversions, represented by the  $\alpha_1^2 a_3 \operatorname{sech}^2(\xi/\tau)$  terms, are identical, even though the initial inversions  $a_3$  and  $a_5$  are not, generally speaking, equal. As a result, inversions  $w_{21}$  and  $w_{32}$  are not, in general, proportional to each other.

One can show by appropriate substitutions that in the cascade case, solutions (23) characterized by  $\alpha_1^2 + \alpha_2^2 = 1$ , result in a contradiction ( $\beta = -1$ ). Thus, three-level simulton propagation is impossible in a cascade system when the amplitudes satisfy  $\alpha_1^2 + \alpha_2^2 = 1$ . The requirement of compatibility of the solutions (23) and (21) of the three-level Bloch equations with the Maxwell equations (18) has thus established that only generalized Cook-Shore pulses with  $\alpha_1^2 + \alpha_2^2 = 4$  will propagate as simultons in a cascade medium.

The contradiction of the negative  $\beta$  can be eliminated if a sign in one of the Maxwell equations is changed. Such a change corresponds to a change in atomic configurations.<sup>14</sup> To be specific, let us assume that we are dealing with the  $\Lambda$  configuration of levels. This changes the sign in Eq. (18b). Substituting the solutions (23) characterized by  $\alpha_1^2 + \alpha_2^2 = 1$  into the appropriate Maxwell equations for the  $\Lambda$  configuration, we obtain again (26) as a definition of  $\tau$  (or  $V$ ), and get the condition

$$\beta = 1 . \quad (29)$$

It is interesting to note that, in this case, there is only one condition involving Rabi frequencies, namely, (24). On the other hand, the Bloch-Maxwell compatibility requirement resulted in condition (29), which involves medium parameters only (we are on resonance so carrier frequencies are equal to atomic transition frequencies). This implies that for certain dipole-allowed transitions in the medium the simulton propagation of the form assumed here (20) and (23) will not be possible, regardless of particular values of the amplitudes  $\alpha_1$  and  $\alpha_2$ . Appropriate dipole-allowed transitions potentially able to support the propagation of simultons given by (17) and (20) have to be identified from spectroscopic data.

We should also note that the initial inversions are identical in magnitude. The minus sign in (23d) results from our notation in which, for the  $\Lambda$  configuration, the condition  $w_{32} > 0$  represents the situation where the *lower* energy level is more strongly populated. The terms representing changes in inversions (those involving  $\operatorname{sech}^2$ ) are, in this case, different in magnitude. This situation is the opposite of what we saw for the cascade case, where the initial inversions were different and the inversion changes the same. The net result, however, is similar: the two inversions are not, generally speaking, proportional to each other.

The fact that  $a_3 = -a_5$  in the  $\Lambda$  case precludes the possibility of simulton propagation in an absorber that was initially in the ground state. The minimum possible initial inversion is only  $a_3 = -\frac{1}{2}$ .

It is easy to show that the possibility of simultons characterized by  $\alpha_1^2 + \alpha_2^2 = 4$  has to be ruled out for the  $\Lambda$  configuration. This can be done, as before, by requiring the consistency between Bloch and Maxwell equations and arriving at the condition  $\beta < 0$ .

It is also easy to show that solutions (23) characterized by  $\alpha_1^2 + \alpha_2^2 = 1$  are also appropriate for the  $V$  configurations. Most of the above discussion for the  $\Lambda$  configuration still holds for the  $V$  configuration. It is interesting to note that, for the  $V$  configuration, simulton solutions (17) and (20) will be supported by a medium initially in the ground state (all population in level 2). Moreover, the range of possible inversions is larger than in the previous case.

Looking at the amplitude condition (24) we see that for  $V$  and  $\Lambda$  configurations the areas of both individual pulses of the simulton will be always smaller than  $2\pi$ . On the other hand, for the cascade configuration, as implied by (22), at least one of the areas of the individual pulses of a simulton will be greater than  $2\pi$ . Thus, the areas implicated by (22) or (24) will be, in general, quite distinct from the  $2\pi$  area of a two-level self-induced-transparency soliton.

One can show that the cascade solutions (21) imply that  $r_{22} = \text{const}$  throughout the entire interaction. That fact, clearly, has been derived and not assumed. However, it may be interesting to note that a restricted case of the coupled Maxwell-Bloch equations may be treated if the condition  $r_{22} = \text{const}$  is imposed at the beginning. In the remaining two configurations  $r_{22}$  does not remain unchanged for the solutions (23).

#### IV. SIMULTONS: NUMERICAL EXPERIMENTS

In Sec. III we have predicted that the two different-wavelength sech pulses given by (17) and (20a) will be able to propagate in a lossless and shape-preserving manner through a three-level atomic medium, provided that the medium and the pulses are prepared in an appropriate way. These simultaneous optical solitons, or simultons, and the corresponding atomic dynamics, have been shown to be solutions of the on-resonance three-level Bloch equations and the reduced Maxwell equations (without phase variation). It should be remarked that the on-resonance assumption is not very restrictive. With pulses that are short enough, one is in the so-called sharp-line regime, where the entire atomic line is excited because the pulse Fourier transform is very broad.

Now we consider the results of numerically modeling the propagation of two specific incident sech pulses in a lossless medium. At the entry face of the medium ( $z=0$ ) the pulses are simultaneous and identical: they have the same pulse lengths  $\tau_a = \tau_b = \tau = 0.333$  in arbitrary units, their peaks coincide, and the peak Rabi frequencies are

$$\Omega_a = \Omega_b = \sqrt{2} \frac{2}{\tau}.$$

The individual area of each pulse is  $\sqrt{2}(2\pi)$ . We have taken, for the sake of simplicity,  $\beta=1$ . The Doppler widths are identical and equal:  $\Delta_{12,23}^D$

$= 1.0$ . (Doppler width is defined as full width at half maximum). The full width of each pulse's Fourier transform is  $\sim 5.033$ , enough larger than 1.0 that we are close to having a pure sharp-line case. The medium is prepared in a mixed initial state with no off-diagonal coherence, and with equal initial inversions. These initial conditions are achieved by choosing the following initial populations:  $r_{11} = \frac{2}{3}$ ,  $r_{22} = \frac{1}{3}$ ,  $r_{33} = 0$ .

The results of numerically modeling this propagation problem are shown in Fig. 2. The manner in which the information is presented in Fig. 2 will be adopted throughout this paper. Each column shows the temporal behavior (of the pulses and of the level populations) in a given cross-sectional plane of the absorber. The propagation distance (from the entry face at  $z=0$ ) is measured in units of the inverse low-signal inhomogeneous absorption length defined by

$$\alpha = G_a \pi g_D(0), \quad (30)$$

where  $g_D(\Delta)$  is the distribution of atomic detunings corresponding to the distribution of atomic velocities mentioned below (13). The bottom member of the column shows the two pulses (of carrier frequencies  $\omega_a$  and  $\omega_b$ , labeled 1 and 2, respectively) as a function of the local time variable  $\zeta = t - z/c$ . The vertical scale shows the real parts of the Rabi frequencies. In Fig. 2 the envelopes of pulses 1 and 2 satisfy simulton conditions, as well as  $\beta=1$ ,

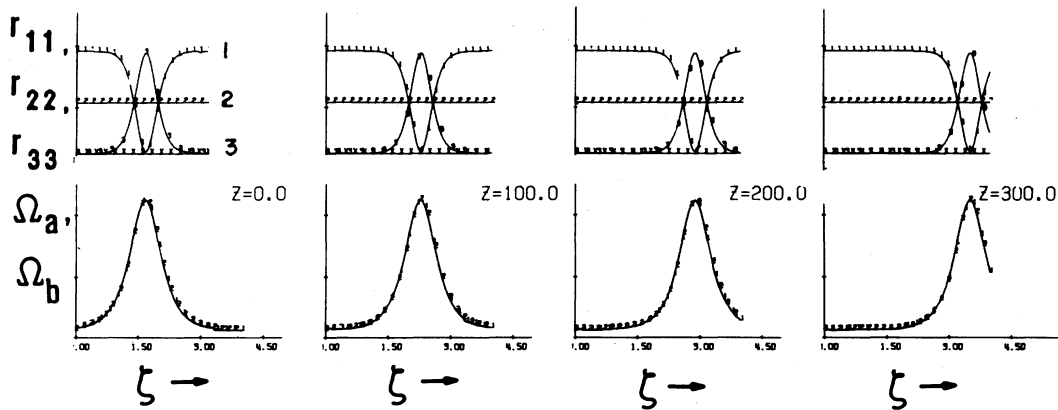


FIG. 2. Simple example of simulton propagation. Each column shows the temporal behavior of the pulses and of the level populations in a given cross-sectional plane of the absorber. The propagation distance (from the entry face at  $z=0$ ) is measured in units of the inverse low-signal inhomogeneous absorption length, defined by Eq. (30). The bottom member of the column shows the two pulses (of carrier frequencies  $\omega_a$  and  $\omega_b$ , labeled 1, and 2, respectively) as a function of the local time variable  $\zeta = t - z/V$ . The vertical scale shows the real parts of the Rabi frequencies. Above each graph of the pulses we show the atomic populations for the resonant atomic levels, labeled 1, 2, and 3, respectively. Incident sech pulses have individual areas  $\sqrt{2} 2\pi$ . Initial populations are  $r_{11} = \frac{2}{3}$ ,  $r_{22} = \frac{1}{3}$ , and  $r_{33} = 0$ .



and are not distinguishable in the graphs. Above each graph of the pulses we show the atomic populations for the resonant atomic levels, labeled 1, 2, and 3, respectively. The propagation distances for the columns are marked in the top right-hand corners of the plots of the pulses. Figure 2 contains four of the columns described above.

Figure 2 clearly demonstrates that the different-wavelength hyperbolic secant pulses found in Sec. III do indeed propagate in a lossless and shape-preserving manner in a three-level medium. The medium may be inhomogeneously broadened, as long as the sharp-line conditions are realized, and the pulses and medium are prepared in the appropriate manner. The on-resonance analytic description utilized in Sec. III is thus shown to be adequate within the limitations of the sharp-line regime.

Note further that the two pulses propagate together and experience a delay (relative to the light line  $z = ct$ ) that linearly increases with propagation distance. That is, the peak of the simulton is later in time at later  $z$  positions. One can be more quantitative at this point. We can define the delay in propagating through a distance  $L$  to be  $\tau_d \equiv (1/V - 1/c)L$ . Then, in the present example, from (26) and (30), we find

$$\begin{aligned} \tau_d &= \frac{1}{2} G_a \tau^2 L w_{21}(\xi = -\infty) \\ &= \frac{1}{6} (\alpha L) \left[ \frac{\tau}{T_2^*} \right] \tau, \end{aligned} \quad (31)$$

where  $T_2^*$  is the usual<sup>1</sup> inhomogeneous lifetime. The same quantity can be estimated from Fig. 2. Both the numerical and theoretical values give

$\tau_d \sim 1.87$ . The agreement is certainly satisfactory. It seems appropriate to point out that, due to the presence of  $w_{21}(\xi = -\infty)$  in (31), simultons will travel faster and experience smaller delays than the pulses of ordinary two-level self-induced-transparency theory. In Fig. 2 the delay is three times smaller. The atomic dynamics at the entry face, represented here by the three on-resonance populations, shows behavior characterized by a full "rotation" of the initial state from  $r_{11} = \frac{2}{3}$ ,  $r_{22} = \frac{1}{3}$ , and  $r_{33} = 0$  to  $r_{11} = 0$ ,  $r_{22} = \frac{1}{3}$ , and  $r_{33} = \frac{2}{3}$ , when the pulses are at their (coincident) peaks, and by the return of the atom to its initial state after the pulses have passed. Owing to the fact that we are in the sharp-line regime, the on-resonance populations and their respective Doppler averages are almost identical at all times. One should also note that the population of level 2, for the case under consideration, remains constant during the entire pulse-atom interaction. The populations  $r_{11}$  and  $r_{33}$ , on the other hand, are at all times symmetric with respect to  $r_{22}$ . All those features remain unaltered during the propagation.

Next, in Fig. 3, we show the propagation of simultaneous identical incident pulses of temporal profiles different from sech. The individual pulse areas are close to  $\sqrt{2}(2\pi)$ , the Doppler widths are again 1.0, and the pulse lengths  $\sim 0.3$ . For such pulses we are even further into the sharp-line regime that was the case for the sech pulses of the previous example. Figure 3 displays results obtained with (top) Gaussian and (bottom) super-Gaussian {with initial temporal behavior of the type  $\Omega \sim \exp[-\frac{1}{2}(t/\tau)^{2n}]$ , where  $n > 1$ } pulses, for propagation distances up to  $\alpha z = 300$ . We note

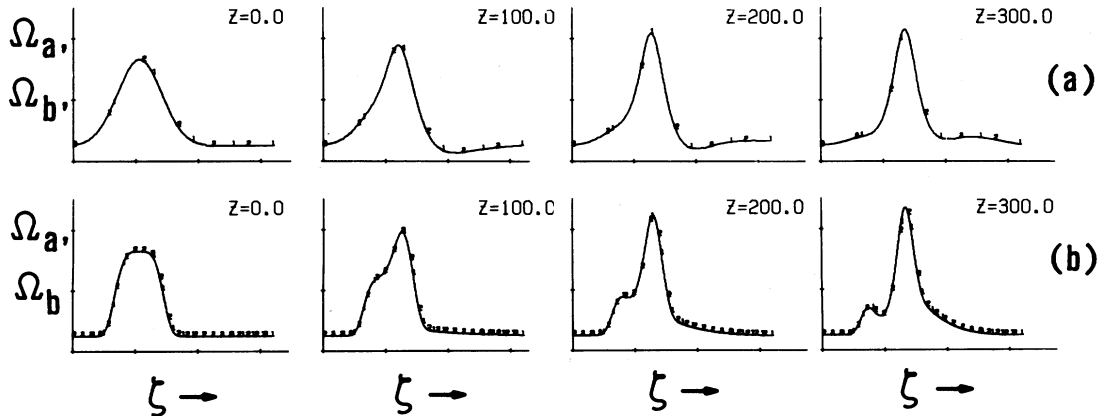


FIG. 3. Simultaneous propagation of (a) Gaussian and (b) super-Gaussian pulses. Parameters are the same as in Fig. 2.

that deviations from the incident sech shape of Fig. 2 result in visible asymmetries between the leading and trailing parts of the propagating pulses. For the super Gaussian the asymmetry is stronger and takes the form of modulation of the leading edge of the pulse. It is interesting to note that, for a given propagation distance, in spite of the fact that the temporal profiles of the pulses differ in their details, the position of the (main) peak is approximately the same for the Gaussian and for the super Gaussian. The peaks experience a delay that is approximately linear, like that given by expression (31). Thus, an interpretation of those results as showing evolution toward a stable sech forms seems plausible. The ringing can be regarded as a  $0\pi$  area pulse superimposed on the emerging sech form. Throughout the entire interaction the pulses still travel and evolve together, although they did not start as sech pulses. One should also remark that the population in level 2 still remains  $\frac{1}{3}$  at all times, and the symmetry between  $r_{11}$  and  $r_{33}$  (with respect to  $r_{22}$ ) is preserved. After the pulse's passage the initial conditions are restored, as was the case in Fig. 2.

In Fig. 4 we display results obtained for super-Gaussian pulses propagating through media characterized by different Doppler broadenings. Case (a) corresponds to  $\Delta_{12,23}^D = 1.0$ , case (b) to

$\Delta_{12,23}^D = 10.0$ , and case (c) to  $\Delta_{12,23}^D = 40.0$ , respectively. The medium's other parameters and its preparation are the same as in the two preceding examples. The pulses used here are the same as those in Fig. 3 (for the super-Gaussian case).

Based on their Fourier widths, both cases (a) and (b) fall within the sharp-line regime. As meaningful comparisons can be made only for physically corresponding propagation distances, we will compare the results in case (b) with those of case (a) for distances (in units of  $\alpha^{-1}$ ) ten times larger.

Indeed, the two cases are quite similar, as far as the pulses are concerned. Some differences will occur between the Doppler averages of the populations of cases (a) and (b), without, however, an appreciable effect on the pulses. For the broader case (c), over distances up to  $\alpha L = 30.0$ , the leading edge modulation seems to be smaller and to be disappearing faster than in the other two cases. The trailing edge ringing is more noticeable in case (c), but it also seems to disappear with propagation. For case (c), the pulses also seem to be more advanced in their evolution toward a sech asymptotic form, as one would expect for a broader-line absorber. In all three cases pulses 1 and 2 still propagate together.

It is interesting to add that, even for case (c), the population  $r_{22}$  and its Doppler average still remain

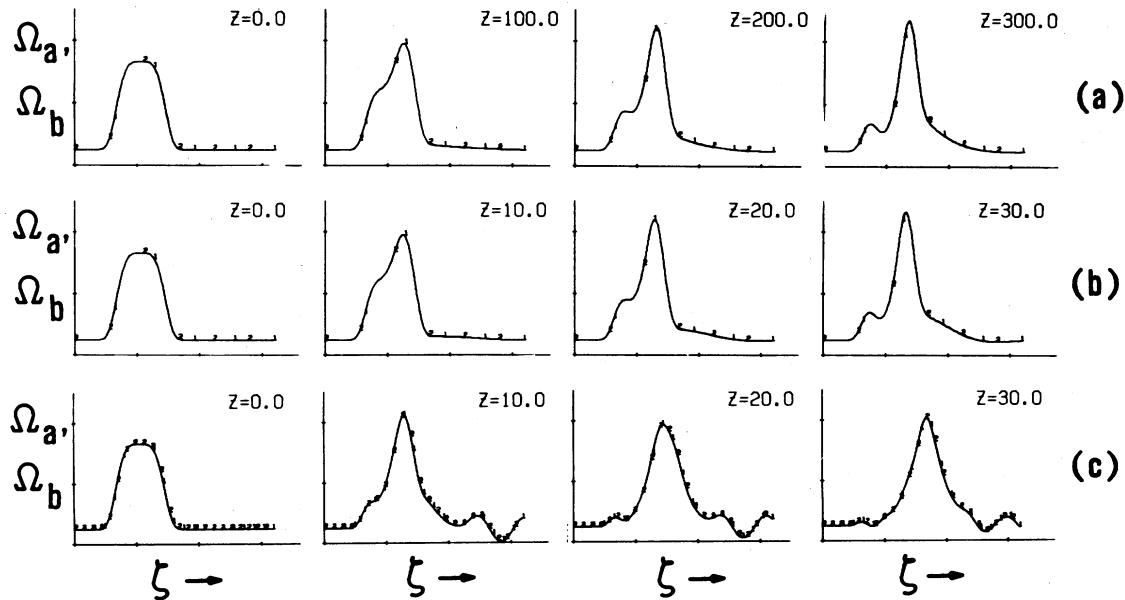


FIG. 4. Propagation of super-Gaussian pulses in media with different Doppler broadening. (a)  $\Delta_{12}^D = 1.0$ ; (b)  $\Delta_{12}^D = 10.0$ ; (c)  $\Delta_{12}^D = 40.0$ . Other parameters same as in Fig. 2.

constant, and the symmetry between  $r_{11}$  and  $r_{33}$ , with respect to  $r_{22}$ , is preserved. It should be noted, however, that the range of changes in the Doppler averages of  $r_{11}$  and  $r_{33}$  is smaller than that of the on-resonance variables. An atom is still left by the pulses in its initial state, in spite of propagation, both in the sense of on-resonance and Doppler-averaged variables.

Figures 2–4 not only demonstrate the validity of the asymptotic sech soliton solutions in the sharp-line regime, but also offer some evidence that such solutions may still be adequate in moderately broad-line cases, and that incident simultaneous pulses with temporal profiles different from sech may still propagate together, while apparently evolving toward the sech form asymptotically. This is more than we can account for analytically (see Sec. III), and it may be suggestive of the possible existence of some global evolution relations analogous to the pulse area-pulse energy formulation of two-level propagation problems.<sup>2,6</sup>

Realizing the limitations of the analytic description currently available, we will adopt a more experimental attitude and pick case (b) of Fig. 4 as a “standard”, with the intention of exploring how sensitive it will be to small changes of parameters such as pulse amplitudes, pulse widths, simultaneous arrival of the incident pulses, and the initial preparation of the medium.

Figure 5 shows how the standard case is influenced by a small deviation from the correct preparation of the medium. Here the initial conditions are  $r_{11}=0.7$ ,  $r_{22}=0.3$ , and  $r_{33}=0$ . Over the propagation distance up to  $\alpha L=120.0$ , the two pulses show some slight differences of amplitude

modulation. It seems, however, that the centers of gravity of the main pulses still travel together. It would certainly be difficult to distinguish the two pulses in practical experimental situations. We may perhaps say that, practically speaking, for the propagation distances of our standard case, the pulses may still be considered as constituting a soliton, in spite of slightly incorrect initial conditions.

One should also note that in the current case the population  $r_{22}$  (and its Doppler average) does not remain constant throughout the interaction. It experiences slight modulation, and, after the pulses’s passage ends up closer to the “correct” value of  $\frac{1}{3}$ . Similarly, the final population in level 1 is slightly less than 0.7, closer to the correct value of  $\frac{2}{3}$ . The modulation of  $r_{22}$  is found to be a characteristic feature in other perturbed cases also. As the other two populations change smoothly, and in a manner reminiscent of the standard case, it seems reasonable to assume that there is a connection between the modulation of  $r_{22}$  and the modulation of the pulse amplitudes.

In Fig. 6 we show the propagation results for the standard case with the following modifications: (top) the initial pulse amplitudes are perturbed by 5% in the opposite directions from the optimum value; (middle) the peaks of two identical pulses are separated by a small fraction of the pulse width, and (bottom) the widths of two pulses of equal amplitudes and coincident peaks differ approximately by 5%. Apart from small details, the character of all three cases is identical, and quite similar to the behavior shown in Fig. 5. The conclusion, clearly, will have to be the same: Although the pulses

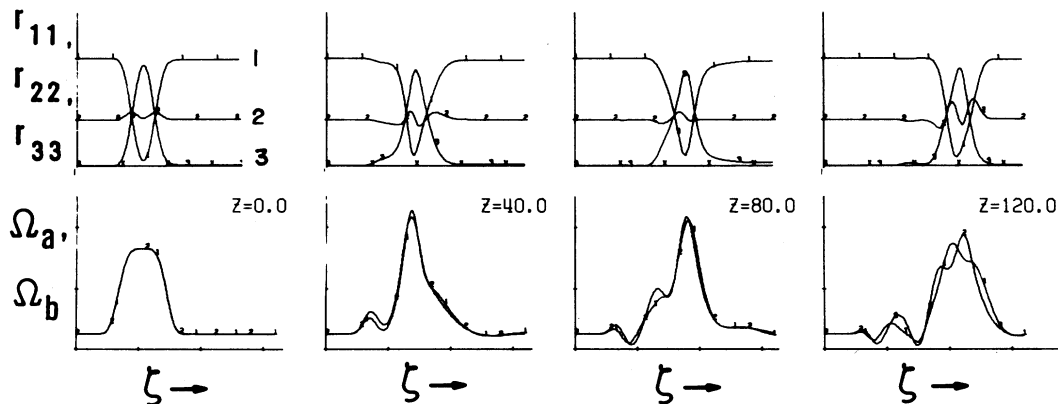


FIG. 5. Propagation for a standard super-Gaussian case with perturbed initial populations ( $r_{11}=0.7$ ,  $r_{22}=0.3$ ,  $r_{33}=0$ ).

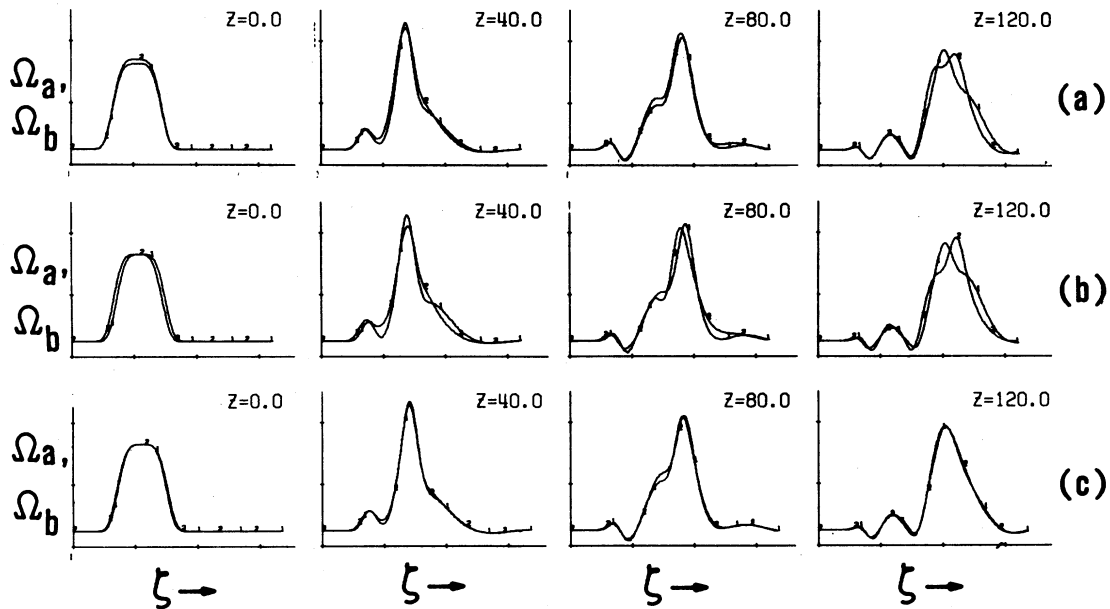


FIG. 6. Propagation in a standard case with small modifications of (a) amplitudes, (b) pulse separations, and (c) pulse widths.

show slightly different modulations, for the propagation distances considered here we can still say that pulses are practically identical and continue to travel together, effectively as a simulton.

We may also remark that although the results shown in Figs. 2–6 have been obtained for  $\beta=1$  and, in particular, for a special choice  $r_f=1$  and  $r_d=1$  ( $r_f=\omega_b/\omega_a$ ,  $r_d=\beta/r_f$ ), it is possible to demonstrate again that other choices  $r_f$  and  $r_d$ , combining to  $\beta=1$ , lead to results that are not appreciably different from the cases reported so far.

Such a situation is clearly more realistic and more attractive from a practical point of view, as it leaves us more freedom in choosing the appropriate transitions capable of supporting simultaneous different-wavelength pulse propagation. We will not, however, display such results here.

Finally, in Fig. 7 we show how the standard case is affected by the presence of atomic relaxation. For simplicity, we allow for relaxation from level 3 to 2, and from 2 to 1 only. The rates of both processes are taken equal for simplicity and denot-

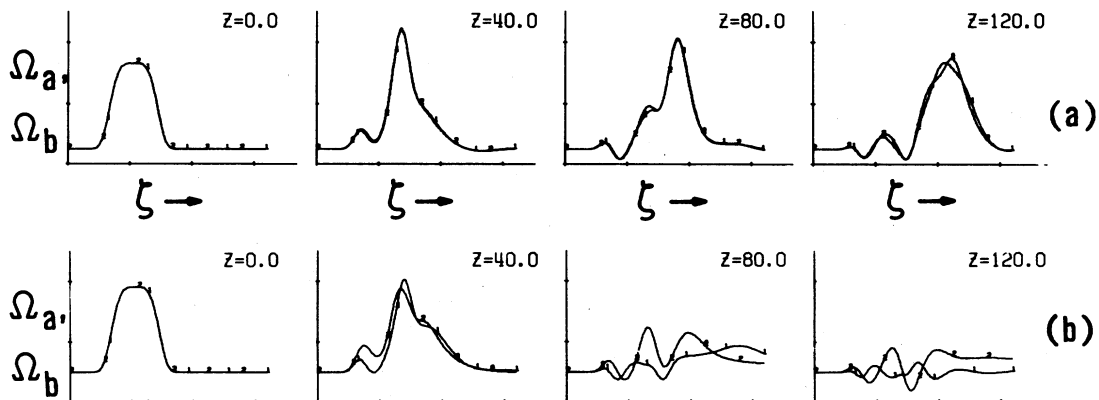


FIG. 7. Effect of internal population-conserving relaxation on the standard case. (a)  $A=0.1$ , and (b)  $A=1.0$ .

ed by  $A$ . The top case, with  $A = 0.1$ , is quite similar to the last two examples reported: the pulses show some modulation but still travel together. The bottom case, with  $A = 1.0$ , shows that simultaneous propagation is disrupted for distances longer than  $az = 40.0$ . It is interesting to note that the usual self-induced-transparency behavior in a compatible case (i.e., amplitude of inversion changes restricted to  $\frac{1}{3}$ ) will be disrupted faster, due to the same rates of coherence decay in both cases, but a faster decay of inversion in the two-level case.

Figure 8 illustrates the situation in which the propagation occurs in a medium whose preparation is substantially different from that required for simultaneous propagation to exist. The medium is assumed to be initially in its ground state. The remaining medium and pulse parameters are the same as in the standard case. For the sake of comparison, we also display in Fig. 8 the earlier results for the standard case. The maximum propagation distance for both prepared and unprepared cases was  $\alpha L = 120.0$ . We see that already for distances  $az \sim 30.0$  the pulses for the unprepared case are quite different in their profiles and velocities. They clearly cease to propagate together. We see that in the unprepared case pulse 2 concentrates most of its energy in a modulated part traveling with the vacuum velocity of light. On the other hand, pulse 1 is delayed. Clearly, due to the "incorrect" preparation, the medium behaves as an absorber initially only for pulse 1, and all features of the simultaneous propagation are rapidly lost.

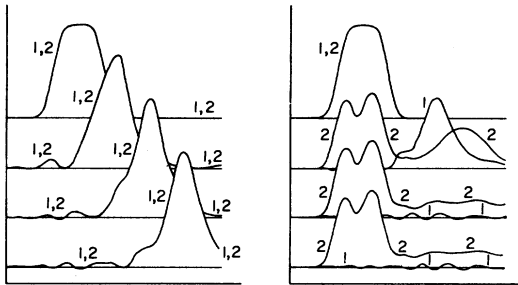


FIG. 8. Standard case propagation in a prepared (left) and unprepared (right) medium. The uppermost profiles show the pulse pairs at the entry face, and each succeeding lower profile shows the results of deeper propagation into the medium. Initial pulse areas are approximately  $\sqrt{2}2\pi$  in all cases. Maximum propagation distance is  $\alpha L = 120.0$ .

All of the results reported so far have dealt with three-level "2 $\pi$ " pulses. It seems worthwhile to investigate the behavior of incident simultaneous pulses of larger areas. Figure 9 shows the results obtained for identical three-level  $4\pi$  pulses in the standard case [the area of an individual pulse is  $\sqrt{2}(4\pi)$ ]. The area has been increased by simply doubling the amplitudes used in the previous standard experiments. The maximum propagation distance is  $\alpha L = 360.0$ . We note that the two pulses still propagate together, and that each of them experiences a breakup into two pulses of different amplitudes, widths, and velocities. Some ringing is also present. The pulses resulting from the breakup could be interpreted as being close to the asymptotic  $\text{sech } \sqrt{2}(2\pi)$  solutions, based on the atomic dynamics (the initial conditions are practically restored after passage of each of the two pulses), and on the fact that the relative delay of two peaks increases approximately linearly with the distance, as would be expected from asymptotic sech solutions [narrower sech pulses have larger amplitudes and travel faster, as can be seen from expression (31)].

Until now our discussion concentrated on the cascade configuration, and specifically on the case characterized by the coupling parameter  $\beta = 1$ . For the sake of completeness, we will also show examples of results for other configurations of energy levels, and for different values of  $\beta$ .

In Figure 10 we display results obtained for a three-level  $2\pi$ -pulse combination when  $\beta = 0.1$ . Other parameters of the problem are

$$\tau_a = \tau_b = 0.333, \quad \Omega_a = 38.139,$$

$$\Omega_b = 12.060, \quad \Delta_{12}^D = \Delta_{23}^D = 1.0.$$

The amplitudes are related by (22), and the initial preparation of the medium is prescribed by (21d) and gives  $r_{11} = 0.524$ ,  $r_{22} = 0.424$ , and  $r_{33} = 0.0$ . The chosen value of  $\beta$  is realized in our case by  $r_f = 1.0$  and  $r_d = 0.1$ . We are again dealing with a sharp-line regime. One can see that the pulses propagate together. Compared with example (a) of Fig. 4, we see that the pulses in the current case behave in a familiar manner but evolve more slowly. This can be attributed to the fact that the amplitude of inversion changes is much smaller for transition  $1 \leftrightarrow 2$  in the current case. We note that the population  $r_{22}$  again remains constant, and that the inversion in transition  $2 \leftrightarrow 3$  is not changing its sign during the entire interaction. We also note

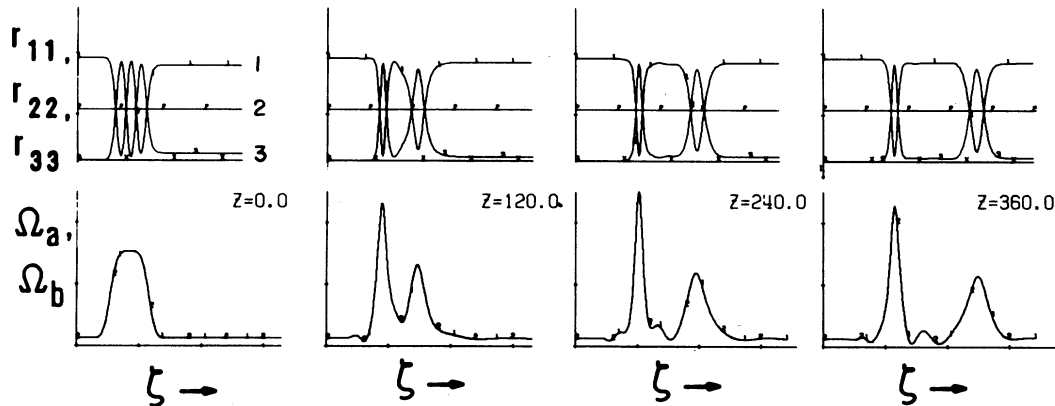


FIG. 9. Simultaneous propagation of a three-level  $4\pi$ -pulse combination in a standard case.

that  $r_{11}$  and  $r_{33}$  are still symmetric with respect to each other, but  $r_{22}$  does not play the role of a symmetry axis any more.

Case  $\beta=0.1$  can also be realized by other combinations of  $r_f$  and  $r_d$ . The possibility  $r_f \neq 1$  is attractive if one is particularly interested in the different-wavelength aspect of the problem. Results obtained do not differ significantly from those of Fig. 10. One should remember, however, that for larger  $r_f$ 's one of the transitions may approach the broad-line regime, while the other still satisfies sharp-line conditions.

Finally, in Fig. 11 we show an example of results obtained for two identical super Gaussians of individual areas  $(1/\sqrt{2})(2\pi)$  propagating in a medium with the  $\Lambda$  configuration of energy levels. The medium is prepared according to (23d) with

the initial populations  $r_{11}=0.5$ ,  $r_{22}=0$ , and  $r_{33}=0.5$ . Parameter  $\beta$  has to be 1.0, as shown in Sec. III. The pulse widths and Doppler widths are the same as in previous standard cases. We are thus in a moderately sharp-line regime. The pulses propagate together and behave in a way similar to that shown in Fig. 4, case (b). Populations  $r_{11}$  and  $r_{33}$  are identical. After the passage of the pulses the initial conditions seem to be restored. One notes that the population of level 2 never exceeds  $\frac{1}{2}$ . It is useful to remember that, in our notation, for the  $\Lambda$  configuration, level 2 has the highest energy. We should also remark that similar results will be obtained for the entire range of values of  $r_f$  and  $r_d$ , compatible with  $\beta=1.0$ , and for unequal pulse amplitudes, as long as condition (24) is obeyed.

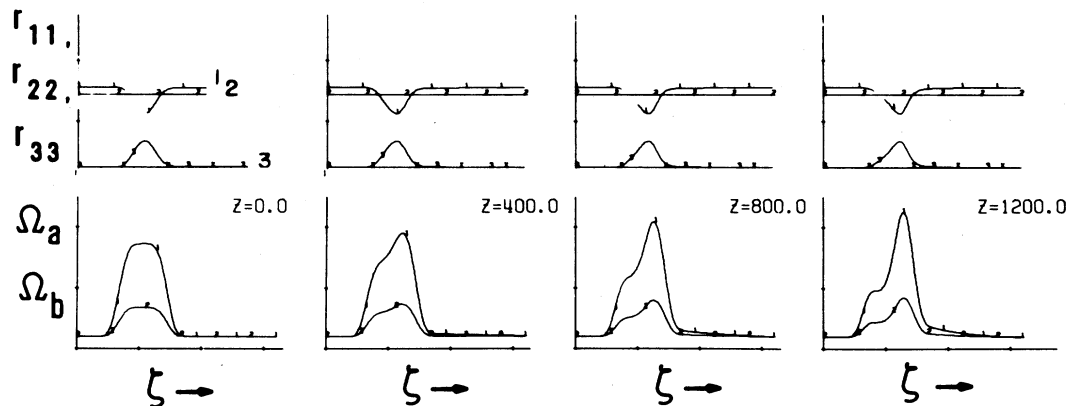


FIG. 10. Sharp-line simultaneous propagation for  $\beta=0.1$ . Pulses and the medium are prepared in a manner described in Sec. III.

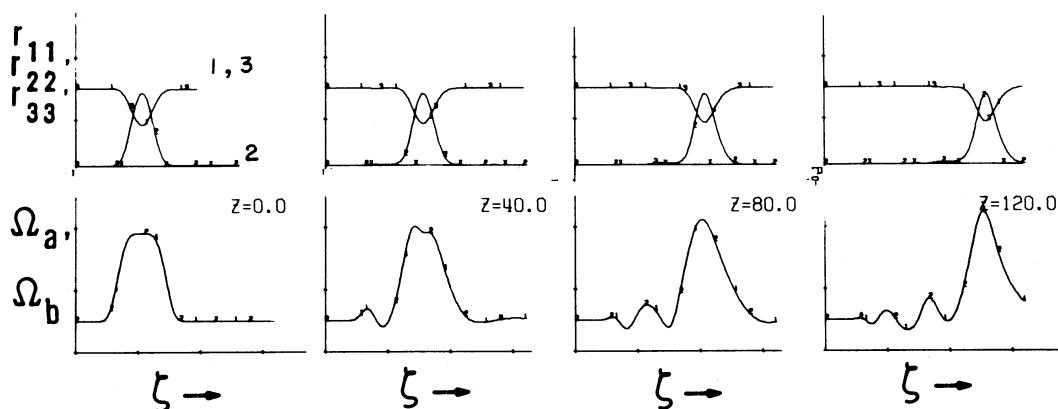


FIG. 11. Simultaneous propagation in a medium of  $\Lambda$  configurations.

## V. DISCUSSION

In Sec. III we have obtained the soliton solutions (21) or (23) to the coupled on-resonance three-level Maxwell-Bloch equations. The solutions are in the form of generalized Cook-Shore pulses, subject to restrictions (22) and (27) or (24) and (29).

We have focused our attention on generalized Cook-Shore pulses only.<sup>8,9</sup> One may argue that such pulses are intuitively attractive as candidates for three-level solitons. This choice allows a particularly simple description of the propagation problem. Concepts can be freely used that have been developed for two-level propagation theory.<sup>1-6</sup> More general multilevel solitons have been found and will be described subsequently.<sup>14</sup> One can now recognize that certain solution pulses known in two-photon self-induced transparency and coherent Raman propagation,<sup>10,11</sup> may also be described as generalized Cook-Shore pulses since they have a common time dependence with possibly different amplitudes. However, those amplitudes are not related by conditions (22) or (24), due to the different nature of those problems.

The two important assumptions characterizing our solutions (on resonance and Cook-Shore form) are certainly limitations on our results. The soliton solutions given by (21) or (23) may, however, merit further attention by the mere fact of their existence. They are the first solutions to the full three-level two-pulse problem obtained without simplifying assumptions about the atomic system such as, for example, the adiabatic elimination of the middle level, commonly used to obtain a

description of two-photon coherent processes.

In order to be able to propagate the solitons described here, i.e., to obtain lossless and shape-preserving propagation of different-wavelength pulses in a three-level medium, one has to perform three tasks. First, one has to obtain spectroscopic information determining the value of  $\beta$ . This is particularly important for  $\Lambda$  and  $V$  configurations, where  $\beta \neq 1$  precludes soliton propagation. Second, one has to prepare the medium in an appropriate initial state. Third, one has to make sure that the input pulses are of the generalized Cook-Shore type. Only an appropriate preparation of both the pulses and the medium will result in soliton propagation.

It should be noted that results (20) and (21) or (23) can be expressed in terms of trigonometric functions of the argument

$$\Theta(\zeta) = \int^{\zeta} \Omega(\xi) d\xi,$$

linear in  $\Omega$ ,<sup>9</sup> whereas arguments of similar trigonometric expressions appearing in two-photon propagation problems are bilinear in the fields or one-photon Rabi frequencies.<sup>10,11</sup> This difference reflects the fact that our problem is "double-photon" rather than two-photon. Another distinction exists between solitons and two-photon self-induced-transparency pulses, which are associated with the two-photon term  $v_{13}$ , while  $u_{13} = 0$ . On the other hand, for soliton pulses, the opposite is true:  $u_{13}$  is the term that matters, although it may vanish for  $\beta = 1$ , and  $v_{13}$  is identically zero. The roles of the  $v_{13}$  and  $u_{13}$  variables can be seen as distinct, in analogy to the one-photon terms:  $v_{12}$  (or  $v_{23}$ ) and  $u_{12}$  (or  $u_{23}$ ) being identified as the absorptive and dispersive components, respectively, of

induced dipole moments. Also, the one-photon terms  $v_{12}$  and  $v_{23}$  are adiabatically eliminated (as are  $u_{12}$  and  $u_{23}$ ) from the description of the two-photon self-induced transparency, while they play an essential role in simulton theory. Clearly, simultons are also distinct from the solitons of the usual one-photon self-induced transparency.

Our numerical experiments show that the ability of different-wavelength pulses to travel together is not seriously impaired, from a practical point of view, by small deviations from the ideal preparation of simulton conditions. It also appears that, although we have developed simulton theory for the sharp-line case (minimal inhomogeneous broadening) a moderate amount of Doppler broadening is not destructive. Examples of pulse evolution toward stable asymptotic forms and of the simultaneous breakup of large-area combinations of pulses may be suggestive of global relations governing multilevel pulse evolution.

#### ACKNOWLEDGMENTS

We acknowledge the interest of, and discussions with, R. J. Cook and B. W. Shore, as well as colleagues at the University of Rochester: P. D. Drummond and F. T. Hioe. This research was partially supported by the U. S. Department of Energy.

#### APPENDIX

We will present below, for the sake of completeness, some details of obtaining the coupled Maxwell-Bloch equations (10) and (14) from equations (3) and (7).

We will not be interested in operators  $\hat{\sigma}_{ij}$  as such, but rather in their expectation values  $\langle \hat{\sigma}_{ij} \rangle$ , which we will denote simply  $\sigma_{ij}$  without a circumflex, for an arbitrary initial state (possibly mixed) of the three-level atom. That initial state is described in terms of a stationary density operator in the Heisenberg picture. By dropping the circumflexes in (7) we obtain appropriate equations of motion for the expectation values  $\sigma_{ij}$ .

Equations of motion (7) can be further simplified if one uses the usual<sup>1</sup> slowly varying envelope representation (SVEA) of the atomic expectation values, and the rotating-wave approximation (RWA). First, we factor appropriate carrier waves out of the  $\sigma_{ij}$ :

$$\sigma_{21}(z,t) = r_{21}(z,t) \exp[i(\omega_a t - k_a z)], \quad (\text{A1a})$$

$$\sigma_{32}(z,t) = r_{32}(z,t) \exp[i(\omega_b t - k_b z)], \quad (\text{A1b})$$

$$\sigma_{31}(z,t) = r_{31}(z,t) \times \exp\{i[(\omega_a + \omega_b)t - (k_a - k_b)z]\}, \quad (\text{A1c})$$

$$\sigma_{ii}(z,t) = r_{ii}(z,t), \quad i = 1, 2, 3 \quad (\text{A1d})$$

$$r_{ij}(z,t) = r_{ji}^*(z,t), \quad i, j = 1, 2, 3. \quad (\text{A1e})$$

Then, in the equations for the slowly varying  $r$ 's, we neglect terms oscillating at optical frequencies. We are led to the following simplified equations of motion involving only slowly varying quantities,  $r_{ij}$  and  $\Omega_{ij}^{a,b}$ :

$$\dot{r}_{12} = -i\Delta_a r_{12} + \frac{i}{2}[\Omega_{21}^a(r_{11} - r_{22}) + \Omega_{23}^b r_{13}], \quad (\text{A2a})$$

$$\dot{r}_{23} = -i\Delta_b r_{23} + \frac{i}{2}[\Omega_{32}^b(r_{22} - r_{33}) - \Omega_{12}^a r_{13}], \quad (\text{A2b})$$

$$\dot{r}_{13} = -i(\Delta_a + \Delta_b)r_{13} + \frac{i}{2}(\Omega_{32}^b r_{12} - \Omega_{21}^a r_{23}), \quad (\text{A2c})$$

$$\dot{r}_{11} = +\frac{i}{2}(\Omega_{12}^a r_{12} - \Omega_{21}^a r_{21}), \quad (\text{A2d})$$

$$\dot{r}_{22} = -\frac{i}{2}(\Omega_{12}^a r_{12} - \Omega_{21}^a r_{21}) + \frac{i}{2}(\Omega_{23}^b r_{23} - \Omega_{32}^b r_{32}), \quad (\text{A2e})$$

$$\dot{r}_{33} = -\frac{i}{2}(\Omega_{23}^b r_{23} - \Omega_{32}^b r_{32}), \quad (\text{A2f})$$

$$r_{ij} = r_{ji}^*, \quad i, j = 1, 2, 3. \quad (\text{A2g})$$

Here the  $t$ - and  $z$ -dependent Rabi frequencies are defined as

$$\Omega_{12}^a = \frac{2}{\hbar}(\vec{d}_{12} \cdot \vec{\epsilon}_a^*) \mathcal{E}_a^*(z,t), \quad (\text{A3a})$$

$$\Omega_{23}^b = \frac{2}{\hbar}(\vec{d}_{13} \cdot \vec{\epsilon}_b^*) \mathcal{E}_b^*(z,t), \quad (\text{A3b})$$

$$\Omega_{21}^a = \frac{2}{\hbar}(\vec{d}_{21} \cdot \vec{\epsilon}_a) \mathcal{E}_a(z,t) = (\Omega_{12}^a)^*, \quad (\text{A3c})$$

$$\Omega_{32}^b = \frac{2}{\hbar}(\vec{d}_{32} \cdot \vec{\epsilon}_b) \mathcal{E}_b(z,t) = (\Omega_{23}^b)^*, \quad (\text{A3d})$$



and  $\Delta_{a,b}$  are the detunings of carrier frequencies  $\omega_a$  and  $\omega_b$  from the respective nearly resonant atomic transition frequencies  $\omega_{21}$  and  $\omega_{32}$ , namely,

$$\Delta_a = \omega_{21} - \omega_a, \quad \omega_{21} > 0 \quad (\text{A4})$$

$$\Delta_b = \omega_{32} - \omega_b, \quad \omega_{32} > 0.$$

Equations (A2) have been written for the cascade configurations of atomic energy levels, with the applied field of the carrier frequency  $\omega_a$  ( $\omega_b$ ) on or near resonance with the allowed dipole transition  $1 \leftrightarrow 2$  ( $2 \leftrightarrow 3$ ). Equations (A2) can be usefully modified

if one expresses the complex quantities  $\Omega_{ij}^{a,b}$  and  $r_{ij}$  ( $i \neq j$ ) in terms of their real and imaginary parts

$$\Omega_{12}^a = R_{12} + iU_{12}, \quad (\text{A5a})$$

$$\Omega_{23}^b = R_{23} + iU_{23}, \quad (\text{A5b})$$

$$r_{kl} = \frac{1}{2}(u_{kl} + iv_{kl}), \quad k > l, \quad l = 1, 2. \quad (\text{A5c})$$

One then obtains the equations of motion (10) involving real quantities only.

\*Present address: Air Force Weapons Laboratory, Kirtland Air Force Base, New Mexico 87117.

<sup>1</sup>L. Allen and J. H. Eberly, *Optical Resonance and Two-Level Atoms* (Wiley, New York, 1975).

<sup>2</sup>S. L. McCall and E. L. Hahn, *Phys. Rev.* **183**, 457 (1969).

<sup>3</sup>R. E. Slusher, in *Progress in Optics*, edited by E. Wolf (North-Holland, Amsterdam, 1974), Vol. 12; F. T. Arecchi, G. L. Masserini, and P. Schwendimann, *Riv. Nuovo Cimento* **1**, 181 (1969); E. Courtens, in *Laser Handbook*, edited by F. T. Arecchi and E. O. Schultz-Du Bois (North-Holland, Amsterdam, 1972), Chap. E5. These are review articles and contain extensive references.

<sup>4</sup>G. L. Lamb, Jr., *Rev. Mod. Phys.* **43**, 99 (1977).

<sup>5</sup>A. Içsevçi and W. E. Lamb, Jr., *Phys. Rev.* **185**, 517 (1969).

<sup>6</sup>S. L. McCall and E. L. Hahn, *Phys. Rev. A* **2**, 861 (1970).

<sup>7</sup>(a) R. G. Brewer and E. L. Hahn, *Phys. Rev. A* **11**, 1641 (1975); (b) D. Grischkowsky, M. M. T. Loy, and P. F. Liao, *ibid.* **12**, 2514 (1975); (c) M. Sargent III and P. Horwitz, *ibid.* **13**, 1962 (1976); (d) R. M. Whitley and C. R. Stroud, Jr., *ibid.* **14**, 1498 (1976); (e) J. R. Ackerhalt and J. H. Eberly, *ibid.* **14**, 1705 (1976); (f) B. W. Shore and J. Ackerhalt, *ibid.* **15**, 1640 (1977); (g) D. Grischkowsky and R. G. Brewer, *ibid.* **15**, 1789 (1977); (h) J. R. Ackerhalt and B. W. Shore, *ibid.* **16**, 277 (1977); (i) J. H. Eberly, B. W. Shore, Z. Bialynicka-Birula, and I. Bialynicki-Birula, *ibid.* **16**, 2038 (1977); Z. Bialynicka-Birula, I. Bialynicki-Birula, J. H. Eberly, and B. W. Shore, *ibid.* **16**, 2048 (1977); (j) P. W. Milonni and J. H. Eberly, *J. Chem. Phys.* **68**, 1602 (1978); (k) J. R. Ackerhalt, J. H. Eberly, and B. W. Shore, *Phys. Rev.*

*A* **19**, 248 (1979); (l) J. H. Eberly and S. V. O'Neil, *ibid.* **19**, 1161 (1979); (m) B. W. Shore and R. J. Cook, *ibid.* **20**, 1958 (1979).

<sup>8</sup>R. J. Cook and B. W. Shore, *Phys. Rev. A* **20**, 539 (1979).

<sup>9</sup>M. Konopnicki, Theory of Coherent Propagation of Short Different-Wavelength Optical Pulses in Three-Level Absorbers, Ph.D. thesis, University of Rochester, Rochester, New York, 1980, available through University Microfilms International, Ann Arbor, Michigan 48106 (unpublished).

<sup>10</sup>N. Tan-no, K. Yokoto, and H. Inaba, *J. Phys. B* **8**, 339 (1975).

<sup>11</sup>N. Tan-no, K. Yokoto, and H. Inaba, *J. Phys. B* **8**, 349 (1975); *Phys. Rev. Lett.* **29**, 1211 (1972); N. Tan-no and K. Higuchi, *Phys. Rev. A* **16**, 2181 (1977); N. Tan-no, T. Shirahata, K. Yokoto, and H. Inaba, *Phys. Lett.* **47A**, 241 (1974); *Phys. Rev. A* **12**, 159 (1975).

<sup>12</sup>C. R. Stroud, Jr., and D. A. Cardimona, *Opt. Commun.* **37**, 221 (1981), and erratum (to be published).

<sup>13</sup>M. J. Konopnicki and J. H. Eberly, *Proceedings of the 10th Annual Simulation and Modeling Conference*, edited by W. G. Vogt and M. H. Mickle (Instrument Society of America, Pittsburgh, 1979), p. 1199

<sup>14</sup>M. J. Konopnicki, P. D. Drummond, and J. H. Eberly, *Opt. Commun.* **36**, 313 (1981); *Bull. Am. Phys. Soc.* **25**, 1124 (1980).

<sup>15</sup>For additional related new conservation relations that provide other constraints on the Bloch variables, see F. T. Hioe and J. H. Eberly, *Bull. Am. Phys. Soc.* **25**, 1125 (1980), and unpublished.

<sup>16</sup>M. J. Konopnicki and J. H. Eberly, *Bull. Am. Phys. Soc.* **20**, 549 (1975).